

Lithium hydride in the early Universe and in protogalactic clouds

Elena Bougleux¹ and Daniele Galli²

¹Dipartimento di Astronomia, Università di Firenze, Largo E. Fermi 5, I-50125 Firenze, Italy

²Osservatorio Astrofisico di Arcetri, Largo E. Fermi 5, I-50125 Firenze, Italy

Accepted Received in original form

ABSTRACT

We examine the processes of formation and destruction of LiH molecules in the primordial gas at temperatures $T \leq 5000$ K in the framework of standard Friedmann cosmological models and we compute the optical depth of the Universe due to elastic Thomson scattering of cosmic background photons on LiH. With the help of a simple model of evolution of a spherical density perturbation we follow the linear growth and the subsequent collapse of protogalactic clouds of various masses, evaluating consistently their physical characteristics and chemical composition. We determine the expected level of anisotropy of the cosmic background radiation due to the presence of LiH molecules in high-redshift protogalactic clouds. We conclude that LiH spectral features generated in the primordial gas are hardly detectable with current techniques and instrumentation.

Key words: early Universe – molecular processes.

1 INTRODUCTION

It has been suggested that a finite amount of molecules such as H₂, H₂⁺, H₃⁺, HD, HD⁺, H₂D⁺, HeH⁺, LiH and LiH⁺ in the primordial gas can induce in the cosmic background radiation (CBR) both *spectral distortions* and *spatial anisotropies* (see Dubrovich 1994 and Maoli 1994 for recent reviews). For example, if the CBR spectrum had some intrinsic distortion in the Wien region originated at high redshift ($z \gtrsim 100$) by whatsoever process of early energy release, then molecules act as heat pumps, absorbing energy in their rotovibrational levels and re-emitting this energy at lower frequencies via rotational transitions (Dubrovich 1977, 1983). Clearly, such a process can occur only if the CBR spectrum deviates from a pure Planck profile. Dubrovich & Lipovka (1995) have performed detailed calculations of this effect for H₂D⁺ molecules: the distortions appear like narrow absorption and emission features in the CBR spectrum.

Spatial anisotropies in the CBR can be produced by Thomson scattering of photons on molecules (or electrons) located in protoclusters moving with a peculiar radial velocity component v_{pec} (Sunyaev & Zel'dovich 1972, 1980; Dubrovich 1977, 1983; Maoli 1994; Maoli, Melchiorri & Tosti 1994). If the abundance of molecules in the primordial gas is sufficiently high, the cumulative effect of elastic Thomson scattering can even create a “curtain” that blurs primordial CBR anisotropies (Dubrovich 1993). The level

of secondary anisotropies in the CBR temperature at a frequency ν is simply

$$\frac{\Delta T}{T} = -\frac{v_{\text{pec}}}{c}(1 - e^{-\tau_{\nu}}), \quad (1)$$

where τ_{ν} is the optical depth at frequency ν through the cloud. The advantage offered by molecules is that they possess much larger photon scattering cross sections (by more than 10 orders of magnitudes) than free electrons. The derivation of the resulting $\Delta T/T$ requires the solution of the equation of radiative transfer in the expanding Universe, described in detail in Appendix A.

In addition, the presence of molecules in protogalactic clouds may induce small fluctuations in the CBR temperature when the population of rotovibrational levels deviates from the equilibrium (Boltzmann) distribution corresponding to the actual radiation temperature T_r . Since the temperature of the gas T_g and the radiation temperature are different for $z \lesssim 10^3$, the populations of molecular levels may differ from a Boltzmann distribution with temperature T_r in clouds of sufficiently high density where collisional excitation processes become significant. The level of anisotropy produced in this case is proportional to the difference between T_r and the excitation temperature of the molecular transition.

The efficiency of the coupling between CBR photons and the primordial gas clearly depends on the chemical composition of the gas, and therefore a description of the

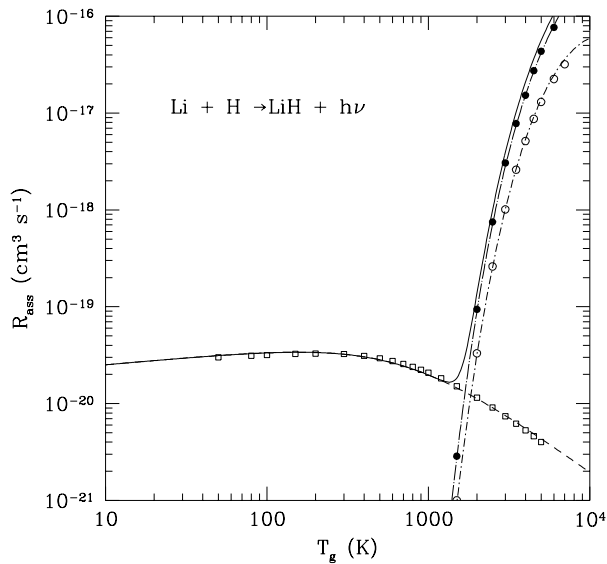


Figure 1. The radiative association rate R_{ass} of LiH as function of the gas temperature T_g . The dashed line shows our fit to the values computed by Dalgarno et al. (1996) and Gianturco & Gori Giorgi (1996a) (squares); the dot long dashed and dot short dashed line our fit to the numerical results by Gianturco & Gori Giorgi (1996b) (solid and empty circles) for the $B^1\Pi \rightarrow X^1\Sigma^+$ and $A^1\Sigma^+ \rightarrow X^1\Sigma^+$ processes respectively. The relative populations of the 2S and 2P levels of Li have been assumed to be at thermal equilibrium with temperature $T_r = T_g$. The solid line shows the total rate.

chemistry of the early Universe is necessary. A large number of papers has been devoted to this problem (e.g. Dalgarno & Lepp 1987; Palla 1988; Puy et al. 1993; Palla, Galli & Silk 1995).

Of all primordial molecules, lithium hydride (LiH) is of considerable interest since the high dipole moment (5.9 debyes) of this molecule makes its rotational and rotvibrational transitions particularly strong (see e.g. Zemke & Stwalley 1980, Bellini et al. 1994, Gianturco et al. 1996). For this reason, the possibility of detecting LiH features in the spectrum of the CBR and in high redshift protogalactic clouds has raised a considerable interest both theoretically (Dubrovich 1994, Maoli 1994, Maoli et al. 1994, Maoli et al. 1996) and observationally (de Bernardis et al. 1993). Specific observational programs are in progress (Signore et al. 1994).

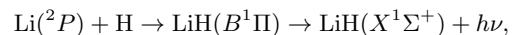
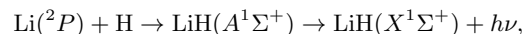
It is important to remind that the abundance of LiH in the pre-galactic gas is proportional to the primordial abundance of Li (hereafter $[\text{Li}/\text{H}]_p$), which is still highly controversial. It was originally shown by Spite & Spite (1982) that the Li abundance on the surface of very metal-poor Pop II stars ($[\text{Li}/\text{H}]_{\text{Pop II}} \simeq 10^{-10}$) is basically independent on metallicity (the so-called Spite plateau). The Pop II value compares well with the abundances of the other light elements predicted by standard big-bang nucleosynthesis and might therefore represent the true primordial Li: $[\text{Li}/\text{H}]_p \simeq [\text{Li}/\text{H}]_{\text{Pop II}} \simeq 2 \times 10^{-10}$. However, evidence is accumulating for a higher primordial value, of the order of $[\text{Li}/\text{H}]_p \simeq 10^{-9}$. From observations made with the Keck telescope of a sam-

ple of sub-giants in the globular cluster M92, Deliyannis, Boesgaard & King (1995) have recently found evidence of significant dispersion in the measured values of $[\text{Li}/\text{H}]_{\text{Pop II}}$ values, strongly suggesting that some amount of depletion has occurred among Spite's plateau stars. If this were the case, then the Li abundance of Pop II stars could be the result of depletion from a higher initial primordial value, a result consistent with the rotating stellar models by Pinsonneault, Deliyannis & Demarque (1992). As a possible way to distinguish between the high- $[\text{Li}]_p$ and the low- $[\text{Li}]_p$ scenarios, Steigman (1996) has recently proposed to determine the ratio of $[\text{Li}/\text{K}]$ from absorption features along different lines-of-sight in the Galaxy and the Large Magellanic Cloud. At the present stage, available data along the line-of-sight of SN1987A favor a primordial abundance of Li lower by at least a factor ~ 2 than the present Pop I value ($[\text{Li}/\text{H}]_{\text{Pop I}} \simeq 1.6 \times 10^{-9}$).

Since the main quantities determined in this study (abundances, optical depths and anisotropies) depend on the assumed initial Li abundance, we should expect an overall increase of their values by an order of magnitude, if the “high” value of $[\text{Li}]_p$ were to be confirmed by future observations.

2 FORMATION AND DESTRUCTION OF LITHIUM HYDRIDE

The LiH molecule has been the subject of a large number of theoretical investigations aimed at determining the conditions for its formation in various astrophysical contexts. Kirby & Dalgarno (1978) (see also Bochkarev & Khersonskii 1985) considered the photodissociation of LiH following absorption from the $v = 0$ vibrational level of the ground $X^1\Sigma^+$ state into the vibrational continuum of the $A^1\Sigma^+$ or $B^1\Pi$ excited states. The cross sections and rates for the inverse radiative association processes



have been recently computed by Gianturco & Gori Giorgi (1996b). Since the $\text{Li}(^2P)$ level lies about 1.85 eV above the $\text{Li}(^2S)$ level, the formation of LiH molecules via electronically excited levels is important only when the temperature is greater than some thousand degrees K. At lower temperatures, processes involving transitions between vibrational levels of the ground $X^1\Sigma^+$ state and its continuum become the dominant mechanisms of radiative association and dissociation of LiH. Such physical conditions are realized in the interior of dense clouds, and in the primordial pre-galactic gas at epoch $z \lesssim 500$.

For the direct radiative association of $\text{Li}(^2S)$ and H,



Lepp & Shull (1984), using semi-classical arguments, estimated a rate coefficient $R_{\text{ass}} \simeq 10^{-17} \text{ cm}^3 \text{ s}^{-1}$, a value adopted in several studies of the chemistry of the early Universe (e.g. Lepp & Shull 1984; Puy et al. 1993; Palla et al. 1995). Khersonskii & Lipovka (1993) performed a fully quantum mechanical calculation analysis of this reaction. Their results show a rapid increase of the cross sections for

Table 1. List of considered reactions

reaction	rate ($\text{cm}^3 \text{s}^{-1}$)	notes	reference
1) $\text{Li}^+ + \text{e} \rightarrow \text{Li} + h\nu$	$1.036 \times 10^{-11} [\sqrt{T_g/107.7} \times (1 + \sqrt{T_g/107.7})^{0.6612} \times (1 + \sqrt{T_g/1.177 \times 10^7})^{1.3388}]^{-1}$	quantal calculation	(a)
2) $\text{Li} + h\nu \rightarrow \text{Li}^+ + \text{e}$		detailed balance applied to (1)	
3) $\text{Li}({}^2S) + \text{H} \rightarrow \text{LiH}({}^1\Sigma^+) + h\nu$	10^{-17} $1.0 \times 10^{-16} T_g^{-0.461}$ $(5.6 \times 10^{19} T_g^{-0.15} + 7.2 \times 10^{15} T_g^{1.21})^{-1}$	semiclassical estimate	(b)
4) $\text{LiH}({}^1\Sigma^+) + h\nu \rightarrow \text{Li}({}^2S) + \text{H}$		quantal calculation	(c)
5) $\text{Li}({}^2P) + \text{H} \rightarrow \text{LiH}({}^1\Sigma^+) + h\nu$	$2.6 \times 10^{-16} T_g^{0.12} \exp(-T_g/6500)$	quantal calculation (adopted)	(d),(e)
6) $\text{LiH}({}^1\Sigma^+) \rightarrow \text{Li}({}^2P) + \text{H} + h\nu$		detailed balance applied to (3)	(f)
7) $\text{Li}({}^2P) + \text{H} \rightarrow \text{LiH}({}^1\Sigma^+) + h\nu$	$1.9 \times 10^{-14} T_g^{-0.34}$	$A^1\Sigma^+ \rightarrow X^1\Sigma^+$, quantal calc.	(f)
8) $\text{LiH}({}^1\Sigma^+) \rightarrow \text{Li}({}^2P) + \text{H} + h\nu$		detailed balance applied to (5)	
9) $\text{Li}^+ + \text{H}^- \rightarrow \text{Li} + \text{H}$	$6.3 \times 10^{-6} T_g^{-1/2} - 7.6 \times 10^{-9} + 2.6 \times 10^{-10} T_g^{1/2}$	$B^1\Pi \rightarrow X^1\Sigma^+$, quantal calc.	(f)
10) $\text{Li} + \text{e} \rightarrow \text{Li}^- + h\nu$	$5.7 \times 10^{-17} T_g^{0.59} \exp(-T_g/17200)$	detailed balance applied to (7)	
11) $\text{Li}^- + h\nu \rightarrow \text{Li} + \text{e}$		experimental cross section	(g)
12) $\text{Li} + \text{H}^+ \rightarrow \text{Li}^+ + \text{H}$	$2.5 \times 10^{-40} T_g^{7.9} \exp(-T_g/1210)$	experimental cross section	(h)
13) $\text{Li} + \text{H}^+ \rightarrow \text{Li}^+ + \text{H} + h\nu$	$1.7 \times 10^{-13} T_g^{-0.051} \exp(-T_g/282000)$	detailed balance applied to (10)	
14) $\text{Li}^- + \text{H}^+ \rightarrow \text{Li} + \text{H}$		quantal calculation	(i)
15) $\text{Li}^+ + \text{H} \rightarrow \text{LiH}^+ + h\nu$	$1.4 \times 10^{-20} T_g^{-0.9} \exp(-T_g/7000)$	quantal calculation	(j)
16) $\text{LiH}^+ + h\nu \rightarrow \text{Li}^+ + \text{H}$		quantal calculation	(d),(e)
17) $\text{LiH}^+ + \text{e} \rightarrow \text{Li} + \text{H}$	$3.8 \times 10^{-7} T_g^{-0.47}$	detailed balance applied to (15)	
18) $\text{LiH}^+ + \text{H} \rightarrow \text{Li} + \text{H}_2^+$	$9.0 \times 10^{-10} \exp(-66400/T_g)$	estimate	(k)
19) $\text{LiH}^+ + \text{H} \rightarrow \text{Li}^+ + \text{H}_2$	3.0×10^{-10}	estimate	(k)
20) $\text{LiH}^+ + \text{H} \rightarrow \text{LiH} + \text{H}^+$	$1.0 \times 10^{-11} \exp(-67900/T_g)$	estimate	(k)
21) $\text{Li} + \text{H}^- \rightarrow \text{LiH} + \text{e}$	4.0×10^{-10}	estimate	(k)
22) $\text{Li}^- + \text{H} \rightarrow \text{LiH} + \text{e}$	4.0×10^{-10}	estimate	(k)
23) $\text{LiH} + \text{H}^+ \rightarrow \text{LiH}^+ + \text{H}$	1.0×10^{-9}	estimate	(k)
24) $\text{LiH} + \text{H} \rightarrow \text{Li} + \text{H}_2$	2.0×10^{-11}	estimate	(k)
25) $\text{LiH} + \text{H}^+ \rightarrow \text{LiH}^+ + \text{H}$	1.0×10^{-9}	estimate	(k)
26) $\text{LiH} + \text{H}^+ \rightarrow \text{Li}^+ + \text{H}_2$	1.0×10^{-9}	estimate	(k)
27) $\text{LiH} + \text{H}^+ \rightarrow \text{Li}^+ + \text{H}_2^+$	1.0×10^{-9}	estimate	(k)

(a) Verner & Ferland (1996); (b) Lepp & Shull (1984); (c) Khersonskii & Lipovka (1993); (d) Dalgarno, Kirby & Stancil (1996); (e) Gianturco & Gori Giorgi (1996a); (f) Gianturco & Gori Giorgi (1996b); (g) Peart & Hayton (1994); (h) Ramsbottom, Bell & Berrington (1994); (i) Kimura, Dutta & Shimakura (1994); (j) Stancil & Zygelman (1996) (k) Stancil, Lepp & Dalgarno (1996).

radiative association with the vibrational quantum number v : the molecule is formed preferentially in vibrational levels with $v = 15-18$. The resulting rate coefficient for the direct radiative association of LiH is in good agreement with the semi-classical estimate of Lepp & Shull (1984) (see Table 1).

More recently, the LiH chemistry in the primordial gas has been reanalyzed in detail by Dalgarno, Kirby & Stancil (1996) and by Stancil, Lepp & Dalgarno (1996, hereafter SLD). The accurate quantal calculation of the radiative association rate of LiH performed by Dalgarno et al. (1996) gives a value of R_{ass} smaller than the one computed by Lepp & Shull (1984) and Khersonskii & Lipovka (1993) by two–three orders of magnitude. The reason for such a large difference is not clear, but it may be related to the approximations adopted by the latter authors. The quantal calculation of R_{ass} for reaction (4) recently performed by Gianturco & Gori Giorgi (1996a) has confirmed SLD’s results to a very high degree of precision. This is even more remarkable, since the two calculations are based on independent sets of potential curves and wavefunctions.

The total rate of radiative association of LiH is represented graphically in Fig. 1 as function of the temperature

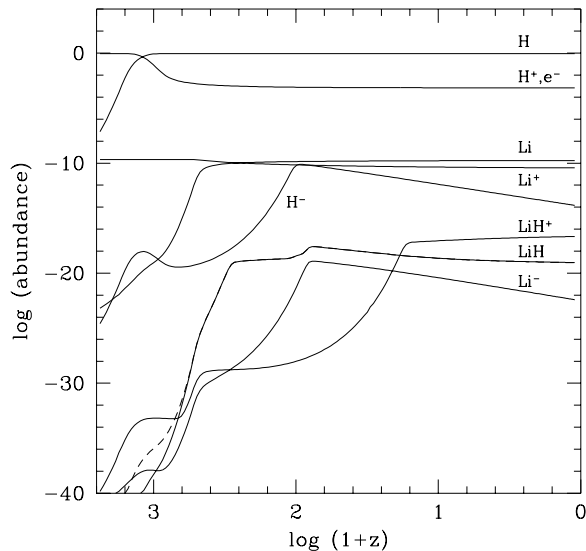
T_g for a gas where the relative populations of the 2S and 2P levels of Li are assumed to be in thermal equilibrium at temperature T_g . It is clear from the Figure that radiative association via excited electronic levels is the dominant formation process of LiH when the gas temperature is larger than ~ 2000 K. Otherwise, LiH is formed only by direct radiative association.

3 CHEMICAL EVOLUTION OF THE PRIMORDIAL GAS

We consider now the chemical evolution of the pregalactic gas in the framework of Friedmann cosmological models. Our standard model is characterized by a Hubble constant $H_0 = 67 \text{ km s}^{-1} \text{ Mpc}^{-1}$ (van den Bergh 1989), a closure parameter $\Omega_0 = 1$, a baryon-to-photon ratio $\eta_{10} = 4.5$ (Galli et al. 1995), and a present radiation temperature $T_0 = 2.726 \text{ K}$ (Mather et al. 1993). The initial fractional abundance of Li nuclei for this model is 2.1×10^{-10} (Smith, Kawano & Malaney 1993). The integration of the chemical network starts at $z = 2500$, with H and Li fully ionized and He fully

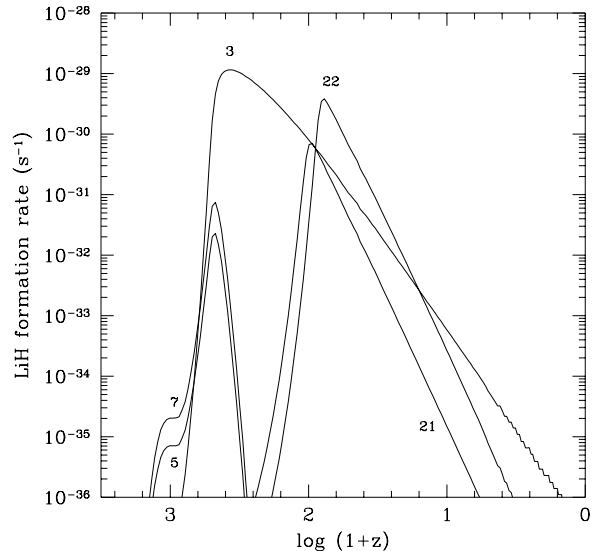
Table 2. Final fractional abundances

$\eta_{10} = 0.7$		$\eta_{10} = 4.5$		$\eta_{10} = 10$	
$z = 10$	$z = 0$	$z = 10$	$z = 0$	$z = 10$	$z = 0$
H^+, e^-	4.6×10^{-3}	4.6×10^{-3}	7.2×10^{-4}	7.1×10^{-4}	3.2×10^{-4}
H^-	1.9×10^{-11}	1.9×10^{-13}	1.5×10^{-12}	1.5×10^{-14}	4.9×10^{-13}
Li	8.2×10^{-10}	8.5×10^{-10}	1.6×10^{-10}	1.7×10^{-10}	8.9×10^{-10}
Li^+	2.8×10^{-10}	2.5×10^{-10}	4.5×10^{-11}	3.8×10^{-11}	2.1×10^{-10}
Li^-	5.0×10^{-20}	4.2×10^{-22}	4.3×10^{-21}	3.9×10^{-23}	1.6×10^{-20}
LiH	1.5×10^{-18}	4.2×10^{-19}	2.2×10^{-19}	9.8×10^{-20}	1.2×10^{-18}
LiH^+	8.1×10^{-17}	1.2×10^{-16}	8.5×10^{-18}	2.2×10^{-17}	2.9×10^{-17}
					1.0×10^{-16}

**Figure 2.** Fractional abundance (by number) of atoms, ions and molecules as function of the redshift for the standard model. The effect of the radiative association of LiH in excited electronic levels is shown by the *dashed* line.

recombined. We have also considered the possibility of a high $[Li/H]_p$, as discussed in the Introduction. If $[Li/H]_p$ is close to 10^{-9} , standard big-bang nucleosynthesis allows either a “low” or a “high” value of η_{10} ($\eta_{10} \simeq 0.7$ or $\eta_{10} \simeq 10$, respectively). The primordial Li abundance predicted by models of inhomogeneous Big Bang nucleosynthesis can even be considerably larger than the values adopted here, but since its value depends sensitively on a number of parameters and assumptions (see e.g. Mathews et al. 1990), for simplicity we consider models based only on standard Big Bang nucleosynthesis results. The initial fractional abundances of H, He and Li are 0.936, 0.064 and 1.1×10^{-9} for the $\eta = 0.7$ model, 0.926, 0.074 and 2.1×10^{-10} for the $\eta = 4.5$ model, and 0.923, 0.077 and 1.1×10^{-9} for the $\eta = 10$ model.

Our chemical network includes about one hundred reactions among 21 chemical species. Reactions involving Li-bearing species and the adopted rates are listed in Table 1. For the recombination rate (reaction 1) we have adopted the accurate fitting formula given by Verner & Ferland (1996), based on the photoionization cross sections computed by Li

**Figure 3.** Processing rates of the most important reactions for the formation of LiH. The curves are labelled with the corresponding reaction numbers listed in Table 1

by Peach, Sarah & Seaton (1988) and Gould (1978). The recombination rate coefficient of Li shown in Table 1 is in good agreement with the results by Caves & Dalgarno (1978).

The evolution of the gas temperature T_g is governed by the equation (see e.g. Galli 1990; Puy et al. 1993; Palla et al. 1995)

$$\frac{dT_g}{dt} = -2T_g \frac{\dot{R}}{R} + \frac{2}{3kn}[(\Gamma - \Lambda)_{\text{Compton}} + (\Gamma - \Lambda)_{\text{mol}}]. \quad (2)$$

The first term represents the adiabatic cooling associated to the expansion of the Universe (R is the scale factor of the Universe). The other two terms represent respectively the net transfer of energy from the CBR to gas (per unit time and unit volume) via Compton scattering of CBR photons on electrons,

$$(\Gamma - \Lambda)_{\text{Compton}} = \frac{4k\sigma_T a T_r^4 (T_r - T_g)}{m_e c} n_e, \quad (3)$$

and via excitation and de-excitation of molecular transitions,

$$(\Gamma - \Lambda)_{\text{mol}} = \sum_{i>j} (n_i C_{ij} - n_j C_{ji}) h \nu_{ij}, \quad (4)$$

where C_{ij} and C_{ji} are the collisional excitation and de-excitation coefficients and n_i are the level populations. The adopted expressions for the radiative and collisional coefficients of LiH as well as the procedure followed to determine the level populations are summarized in Appendix B. For the molecular heating and cooling of the gas we have considered the contributions of H₂, HD and LiH.

When the rate of collisional de-excitation of the roto-vibrational molecular levels is faster (slower) than their radiative decay, the energy transfer function $(\Gamma - \Lambda)_{\text{mol}}$ can become an effective heating (cooling) source for the gas (cf. Khersonskii 1986, Puy et al. 1993). In general, the contribution of molecules to the heating/cooling of the gas becomes important only during the phase of collapse of protogalactic objects (see Sect. 4).

The chemical/thermal network is completed by the equation for the redshift

$$\frac{dt}{dz} = -\frac{1}{H_0(1+z)^2 \sqrt{1+\Omega_0 z}}, \quad (5)$$

where H_0 is the Hubble constant. The density $n(z)$ of baryons at redshift z is

$$n(z) = \Omega_b n_{\text{cr}} (1+z)^3, \quad (6)$$

where n_{cr} is the critical density. The abundance of atoms and molecules is measured with respect to the total number of baryons: $f(\text{H}) = n(\text{H})/n$ and so on.

3.1 Results

The evolution of the fractional abundances of H, H⁺, H⁻, Li, Li⁺, Li⁻, LiH⁺ and LiH for the standard model is shown in Fig. 2 as function of the redshift z . The abundances at $z = 10$ and $z = 0$ for all the models considered are listed in Table 2.

In all models, the final abundance of LiH is extremely small, of the order of 10^{-19} – 10^{-18} . The maximum final abundance ($\sim 5 \times 10^{-19}$) is obtained for the $\eta_{10} = 10$ model. Fig. 3 shows the relative contribution of individual chemical reactions to the formation of LiH in the early Universe. Radiative association from Li(²P) is significant only for $z > 650$, with the process $B^1\Pi \rightarrow X^1\Sigma^+$ being dominant. Otherwise, LiH is formed mostly by radiative association from Li(²S) (reaction 3). At $z \sim 80$ the reactions of associative detachment (21) and, most importantly, (22) also contribute to the formation of LiH. Notice however that although the value of the rate coefficients for the latter reactions is rather uncertain (see SLD), the asymptotic value of the abundance of LiH is largely determined by reaction (3), whose rate is now well established (Dalgarno, Kirby & Stancil 1996, Gianturco & Gori Giorgi 1996a).

The evolution of Li⁻ for $z < 100$ closely mimicks that of H⁻, both ions being removed at low temperature by reactions of mutual neutralization with H⁺ at a rate proportional to $T_g^{-1/2}$. Since $T_g \propto (1+z)^2$ in this range of redshift, the abundances of H⁻ and Li⁻ decrease like $(1+z)$, as shown in Fig. 2. Our computed abundances of H⁺, H⁻, Li and LiH⁺ at $z = 10$ are in excellent agreement with the results

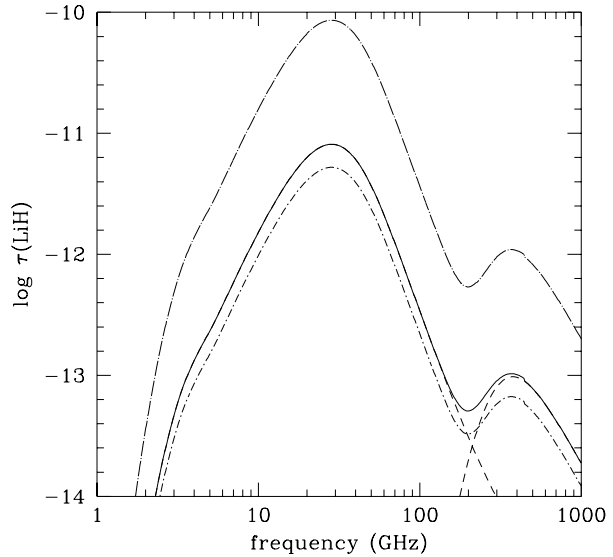


Figure 4. Optical depth of the Universe generated by Thomson scattering of CBR photons on LiH molecules for the standard model (solid curve) and for the high primordial Li cases (dot short dashed curve, $\eta_{10} = 0.7$; dot long dashed curve, $\eta_{10} = 10$). For the standard model, the contribution of rotational and rotovibrational transitions is shown by the dashed curves.

obtained by SLD (within 10–20%), our abundance of Li⁺ being a factor 1.8 smaller. Our values for Li⁻ and LiH at $z = 10$ are smaller by large factors (~ 900 and ~ 300 , respectively) than those published by SLD, but the two computations give essentially the same results when a sign mistake in the rate adopted by SLD for reaction (10) is corrected.

An interesting result is that LiH⁺ is more abundant than LiH for $z \lesssim 18$, by a factor ~ 200 for the standard model. This is in agreement with the early prediction by Dalgarno & Lepp (1987).

3.2 Optical depth

Having obtained the LiH abundance as function of the redshift, we are now able to compute, with the help of the formulae listed in Appendix A, the total optical depth of the Universe due to elastic Thomson scattering of CBR photons on LiH molecules (see eq. [A9]). The result is shown in Fig. 4 as function of the frequency of observation ν . The maximum optical depth for the standard model is $\tau_{\text{LiH}}^{\text{max}} = 6 \times 10^{-11}$, at $\nu^{\text{max}} = 30$ GHz. Pure rotational transitions of the $v = 0$ level dominate at this frequency. The general behaviour of $\tau_{\text{LiH}}(\nu)$ shown in Fig. 4 is in agreement with the one obtained by Maoli et al. (1994). The attenuation of CBR anisotropies being of order τ_{LiH} , little room is left for the “molecular blurring” suggested by Dubrovich (1993). Even for the high [Li/H]_p model with $\eta_{10} = 10$, where a larger optical depth is obtained, the induced attenuation is still insignificant.

Table 3. Physical quantities for a $10^{10} M_{\odot}$ collapsing protogalaxy

t/t_{ff}	z	n (cm^{-3})	T_{g} (K)	R (kpc)	θ ($''$)	v_{coll} (km s^{-1})	v_{pec} (km s^{-1})	$f(\text{H}_2)$	$f(\text{HD})$	$f(\text{LiH})$
0.0	10.00	1.38×10^{-3}	9.6	38.8	28.2	0.0	90	4.5×10^{-6}	5.3×10^{-9}	2.2×10^{-19}
0.1	7.45	1.41×10^{-3}	9.8	38.5	22.8	3.8	103	4.5×10^{-6}	5.4×10^{-9}	2.4×10^{-19}
0.2	6.03	1.49×10^{-3}	10	37.8	19.6	7.6	113	4.6×10^{-6}	5.4×10^{-9}	2.8×10^{-19}
0.3	5.10	1.64×10^{-3}	11	36.6	17.2	12	121	4.6×10^{-6}	5.4×10^{-9}	3.0×10^{-19}
0.4	4.41	1.91×10^{-3}	12	34.8	15.2	16	129	4.6×10^{-6}	5.4×10^{-9}	3.4×10^{-19}
0.5	3.91	2.34×10^{-3}	14	32.5	13.4	21	135	4.7×10^{-6}	5.5×10^{-9}	3.6×10^{-19}
0.6	3.47	3.22×10^{-3}	17	29.2	11.4	27	142	4.7×10^{-6}	5.6×10^{-9}	4.2×10^{-19}
0.7	3.13	4.99×10^{-3}	23	25.3	9.4	33	148	4.8×10^{-6}	5.8×10^{-9}	4.8×10^{-19}
0.8	2.86	9.81×10^{-3}	36	20.2	7.2	45	153	5.0×10^{-6}	6.5×10^{-9}	5.6×10^{-19}
0.9	2.63	3.31×10^{-2}	80	13.4	4.8	65	157	5.8×10^{-6}	9.5×10^{-9}	7.2×10^{-19}
0.95	2.54	1.05×10^{-1}	172	9.15	3.2	85	159	7.9×10^{-6}	1.1×10^{-8}	9.2×10^{-19}

4 A SIMPLE MODEL OF A COLLAPSING PRIMORDIAL CLOUD

So far our attention has been directed exclusively to the global effects of LiH molecules in the *homogeneous* primordial gas. One of the main limitations to the occurrence of detectable features is the low molecular abundance obtained in such a context. It is therefore of interest to follow the chemical (and thermal) evolution of the first density inhomogeneities that emerged from the expanding primordial gas. Those initial density perturbations whose mass exceeded the Jeans mass were unstable to gravitational collapse and evolved to form galaxies and galaxy clusters. The increase in density during the first (quasi adiabatic) phase of collapse can provide suitable conditions for the build-up of considerably larger molecular fraction than in the surrounding expanding Universe. In addition, velocity gradients in a cloud may contribute to enhance the effective optical depth of localized regions in the Universe (Maoli et al. 1994, 1996).

Let us consider then the collapse of a purely baryonic primordial cloud in order to determine the abundance of the relevant molecular species as function of time and to predict the level of anisotropies induced by molecular transitions during the collapse of the cloud. We follow the approach of Lahav (1986) considering a spherical homogeneous cloud of mass M , uniform density n and radius R contracting (or expanding) in a homologous fashion ($v(r) \propto r$). We assume that the radius of the cloud reaches its maximum value at the *turn-around* epoch z_{ta} , when the density and temperature of the cloud are related to the corresponding quantities in the ambient gas by

$$\rho_{\text{ta}} = \left(\frac{3\pi}{4}\right)^2 \rho_{\text{g}}(z_{\text{ta}}), \quad (7)$$

$$T_{\text{ta}} = \left(\frac{3\pi}{4}\right)^{4/3} T_{\text{g}}(z_{\text{ta}}). \quad (8)$$

The radius at turn around R_{ta} is fixed by the mass and density of the cloud. In adiabatic collapse the temperature of the gas in the cloud, T_{g} , increases like R^{-2} .

By virtue of the hypothesis of homologous collapse, the primordial cloud may be treated in the same way as the expanding Universe in the previous Sections. For example, eq. (2) for the gas temperature still holds if one replaces the scale factor of the Universe with the cloud's radius. The optical depth of the cloud by elastic Thomson scattering of

CBR photons on LiH molecules is given again by eq. (A9), but the cosmological velocity gradient is now replaced by the velocity gradient due to gravitational collapse. A more sophisticated calculation of the optical depth, taking into account projection effects, can be found in Maoli et al. (1996).

Defining a non-dimensional radius ξ and temperature θ by

$$R = \xi R_{\text{ta}}, \quad T_{\text{g}} = T_{\text{ta}} \theta \xi^{-2}. \quad (9)$$

the equations for the radius and for the temperature can be written as (Lahav 1986)

$$\frac{d^2\xi}{dt^2} = \frac{5kT_{\text{ta}}}{\mu m_H R_{\text{ta}}^2} \theta \xi^{-3} - \frac{GM}{R_{\text{ta}}^3} \xi^{-2}, \quad (10)$$

and

$$\frac{d\theta}{dt} = \frac{2}{3} \frac{(\Gamma - \Lambda)_{\text{Compton}} + (\Gamma - \Lambda)_{\text{mol}}}{nkT_{\text{ta}}} \xi^2, \quad (11)$$

It is convenient to express time in units of the free-fall time for the cloud,

$$t_{\text{ff}} = \pi \left(\frac{R_{\text{ta}}^3}{8GM}\right)^{1/2}. \quad (12)$$

Once the mass M and the turn-around redshift z_{ta} are fixed, the evolution of the model cloud is determined by the integration of eq. (10) and (11). A relation between M and z_{ta} can be obtained by prescribing the power spectrum of the density perturbations (see e.g. Gunn & Gott 1972, Lahav 1986). For simplicity, we prefer to use a reference value $z_{\text{ta}} = 10$ for all masses.

We consider here a low-mass cloud with $M = 5 \times 10^5 M_{\odot}$, slightly above the Jeans mass at $z_{\text{ta}} = 10$ ($M_J = 3 \times 10^5 M_{\odot}$), and a galactic-size cloud with $M = 10^{10} M_{\odot}$. Fig. 5 shows the time evolution of the cloud's radius, density and temperature (all normalized to their initial turn-around values) for the $M = 5 \times 10^5 M_{\odot}$ case. The evolution is followed for about three free-fall times for illustrative purposes only; in a more realistic model, relaxing the assumption of homologous contraction/expansion, the actual evolution of the cloud is expected to deviate from the one shown here owing to the shocking of different mass shells (see e.g. Haiman, Thoul & Loeb 1996). Because of molecular cooling, the model cloud performs a series of oscillations of decreasing amplitude and period, in striking contrast with the corresponding evolution in the adiabatic case (dashed

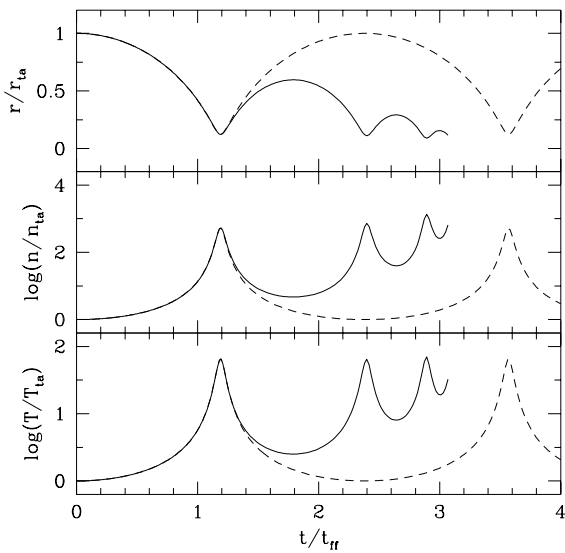


Figure 5. Time evolution of radius, density and temperature for a primordial cloud of mass $M = 5 \times 10^5 M_\odot$. All quantities are normalized to their initial turn around values. Time is in units of the free-fall time. *Dashed lines*: adiabatic evolution; *solid lines*: non-adiabatic evolution.

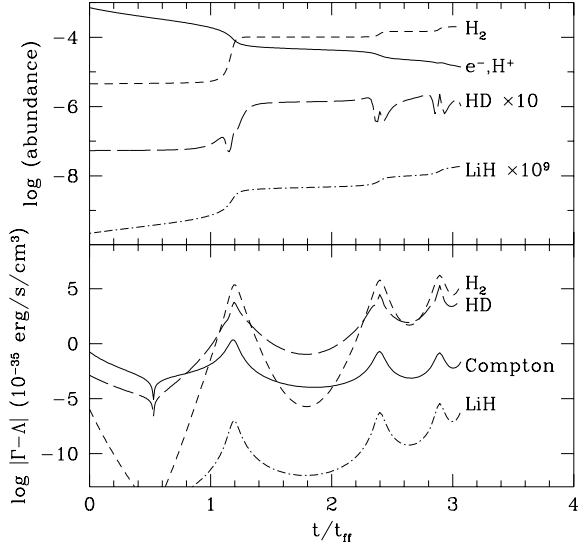


Figure 6. *Upper panel*: fractional abundances of the relevant atomic and molecular species as function of time for the same primordial cloud as in Fig. 5. *Lower panel*: absolute value of the net energy transfer due to molecular and Compton heating/cooling processes.

lines). Fig. 6 shows the fractional abundance of the relevant atomic and molecular species and the net energy exchange between gas and radiation due to molecular and Compton processes, for the same case as in Fig. 5. Both processes act as a net heating for the cloud for $t < 0.53 t_{\text{ff}}$, when $T_r > T_g$, and as a net cooling afterwards. It is important to notice the relevant role played by HD molecules, in addition to H_2 , for cooling the gas during the early phases of collapse. As shown in Fig. 6, heating/cooling by LiH molecules is negligible at all times.

The relevant physical characteristics during the collapse of the $M = 10^{10} M_\odot$ cloud are summarized in Table 3. The listed quantities are: redshift z , cloud density n , temperature T_g , radius R , angular diameter θ , collapse velocity v_{coll} of the outermost shell, peculiar velocity v_{pec} , and fractional abundances of the most relevant molecular species. The angular diameter θ of a spherical cloud of proper radius R at redshift z is computed from the formula (see e.g. Peebles 1971)

$$\theta(R, z) = \frac{H_0 R}{c} \frac{\Omega_0^2 (1+z)^2}{\Omega_0 z + (\Omega_0 - 2)(\sqrt{1 + \Omega_0 z} - 1)}. \quad (13)$$

For the peculiar velocity we follow Maoli et al. (1994) assuming the simple law of evolution of velocity dispersion in the linear regime (see e.g. Peebles 1980)

$$v_{\text{pec}}(z) = \frac{v_{\text{pec}}(0)}{\sqrt{1+z}}, \quad (14)$$

where $v_{\text{pec}}(0) = 300 \text{ km s}^{-1}$ is the present-day galaxy velocity dispersion (Peebles 1993). We assume that this velocity is directed along the line of sight. Table 4 shows the value of the optical depth of the three lowest rotational transitions of LiH as function of time, computed according to eq. (A9).

Anisotropies of the CBR generated by the peculiar motion of the protogalactic cloud can be positive or negative depending on whether the cloud is approaching or receding (see eq. [1]). Although the total peculiar velocity of a collapsing cloud results from the combination of v_{pec} and the collapse velocity v_{coll} , we see from the values listed in Table 3 that the latter can be neglected for most of the collapse phase. For a perturbation evolving in a homologous way, the instant of turn around, when the radial collapse velocity exactly compensates the overall cosmological expansion, presents interesting peculiarities. At this time, in fact, all the molecules in the cloud are “at rest”, and they all contribute to the optical depth. Similar considerations hold for the line width: at the redshift of turn-around the width of a line is the thinnest, practically equal to the thermal width $(\Delta\nu/\nu)_{\text{th}}$. This effect was originally predicted by Zeldovich (1978), who pointed out that weak and narrow spectral features generated in protogalaxies (or protoclusters) reaching their radii of turn-around could be superimposed to the spectrum of the CBR.

5 DISCUSSION AND CONCLUSIONS

The presence of LiH in collapsing protogalactic clouds may induce fluctuations of the CBR brightness temperature on scales of $\sim 10''$ which can be in principle revealed by the use of arrays of telescopes and aperture synthesis techniques. However, it is clear from the values of τ_{LiH} listed in Table 4 that the expected spectral features of LiH in protoclusters are

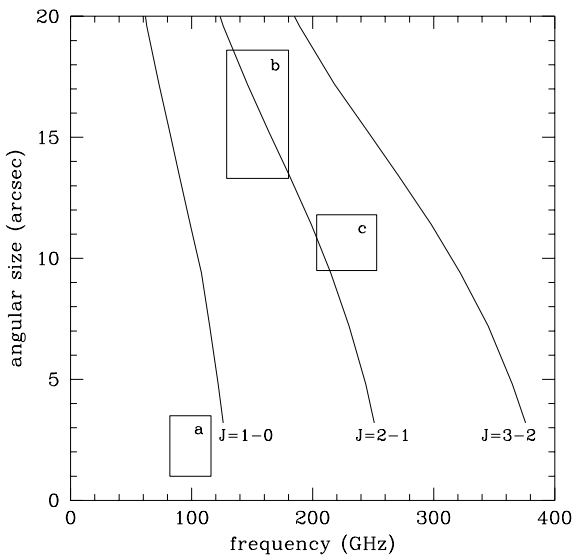


Figure 7. Relation between the angular size θ of a $10^{10} M_{\odot}$ collapsing cloud and the redshifted frequency ν of the three lowest rotational transitions of LiH. Boxes represent indicatively regions of the plane $\nu-\theta$ that can be explored with current telescopes: IRAM Plateau-de-Bure Interferometer (a), IRAM 30 m (b and c).

extremely weak: the associated anisotropies in the CBR temperature, according to eq. (1) are completely negligible during most of the collapse phase. Although the optical depth rises very rapidly towards the end of the collapse phase, the resulting value of $\Delta T/T$ cannot be predicted quantitatively on the basis of the simple model adopted in this work, and a more realistic approach should be taken.

The relation between the angular size θ of the model cloud and the redshifted frequencies of the three lowest rotational transitions of LiH is shown in graphic form in Fig. 7, where the coverage of the plane $\nu-\theta$ of current telescopes is also schematically displayed. Probably the most appealing observational prospective is to search for CBR temperature fluctuations associated with the $J = 1-0$ rotational transition of LiH in “evolved” protogalaxies with the IRAM Plateau-de-Bure Interferometer at 3 mm. Although the actual level of temperature fluctuations is hard to predict quantitatively for such evolved objects, it might be close to the sensitivity limit of this instrument. It is also important to remind that the values of $\Delta T/T$ obtained above are proportional to the assumed value of the primordial abundance of Li (the results presented above are obtained with $[\text{Li}/\text{H}]_p = 2.1 \times 10^{-10}$).

The main conclusions of our study are:

(a) due to its low rate of radiative association, the final abundance of LiH is very small and the molecule is only a minor constituent of the primordial gas. In our standard model, characterized by $H_0 = 67 \text{ km s}^{-1} \text{ Mpc}^{-1}$, $\eta_{10} = 4.5$, $\Omega_0 = 1$, the abundance is $f(\text{LiH}) \simeq 10^{-19}$ at $z = 10$. Such a low value casts serious doubts about the use of LiH as a probe of the physical conditions of the gas at very high redshift. These findings reinforce the conclusions reached by

Table 4. Optical depth of the first three rotational transitions of LiH for a $10^{10} M_{\odot}$ collapsing primordial cloud

t/t_{ff}	τ_{10}	τ_{21}	τ_{32}
0.0	2.8×10^{-10}	4.2×10^{-10}	1.8×10^{-10}
0.1	1.5×10^{-11}	1.6×10^{-11}	4.4×10^{-12}
0.2	1.1×10^{-11}	9.6×10^{-12}	1.7×10^{-12}
0.3	1.0×10^{-11}	7.0×10^{-12}	8.6×10^{-13}
0.4	1.1×10^{-11}	6.2×10^{-12}	5.4×10^{-13}
0.5	1.2×10^{-11}	5.6×10^{-12}	3.6×10^{-13}
0.6	1.4×10^{-11}	5.6×10^{-12}	2.6×10^{-13}
0.7	1.9×10^{-11}	6.4×10^{-12}	2.2×10^{-13}
0.8	2.8×10^{-11}	8.2×10^{-12}	2.2×10^{-13}
0.9	5.8×10^{-11}	1.5×10^{-11}	3.0×10^{-13}
0.95	1.2×10^{-10}	3.0×10^{-11}	1.4×10^{-12}

SLD in a similar analysis. The abundance of LiH^+ for $z \lesssim 18$ is about two orders of magnitude larger than the abundance of LiH.

(b) Taking into account the possibility of a higher value of $[\text{Li}]_p$, the final abundance of LiH and LiH^+ may increase up to $\sim 10^{-18}-10^{-17}$.

(c) The estimate of the optical depth due to resonant scattering of the CBR photons on LiH molecules yields a value of $\tau_{\text{LiH}}^{\text{max}} \sim 10^{-11}-10^{-10}$ at a frequency of 30 GHz. Most of the contribution to the optical depth comes from rotational transitions between high J levels. The attenuation of pre-existing anisotropies of the CBR is therefore completely negligible.

(d) The enhancement of the LiH abundance during the collapse of protogalactic clouds gives rise to fluctuations in the temperature of the CBR associated with the peculiar motion of the object. For a $10^{10} M_{\odot}$ protogalactic cloud reaching its turn-around at $z_{\text{ta}} = 10$, the expected level of anisotropy is far too low to be of any observational relevance during most of the collapse phase. The actual abundance of LiH in the latest phases of collapse cannot be quantitatively predicted by the methods presented here.

Acknowledgements

We thank Riccardo Cesaroni, Roberto Maoli and Francesco Palla for useful comments and conversations. We wish to thank in particular Dr. Paola Gori Giorgi for making her work available to us in advance of publication and for a large number of clarifying discussions.

REFERENCES

Bellini, M., de Natale, P., Inguscio, M., Fink, E., Galli, D., Palla, F. 1994, *ApJ*, 424, 507
 Bochkarev, N. G., Khersonskii, V. K. 1985, *Bull. Obs. North Caucasus*, 18, 84
 Caves, T. C., Dalgaard, A. 1972, *J. Quant. Spectrosc. Radiat. Transfer*, 12, 1539
 Dalgaard, A., Lepp, S. 1987, in *Astrochemistry*, IAU Symposium 118, eds. M. S. Vardya & S. P. Tarafdar, Reidel, p. 109
 Dalgaard, A., Kirby, K., Stancil, P. C. 1996, *ApJ*, 458, 397
 Davies, D. W. 1986, *Chem. Phys. Lett.*, 128, 315
 de Bernardis, P., Dubrovich, V. K., Encrenaz, P., Maoli, R., Masi,

S., Mastrantonio, G., Melchiorri, B., Melchiorri, F., Signore, M., Tanzilli, P. E. 1993, *A&A*, 269, 1

Deliyannis, C. P., Boesgaard, A. M., King, J. R. 1995, *ApJ*, 452, L13

Dubrovich, V. K. 1977, *SvA Lett.*, 3, 181

Dubrovich, V. K. 1983, *Bull. Spec. Astrophys. Obs. North Caucasus*, 13, 31

Dubrovich, V. K. 1993, *SvA Lett.*, 19, 53

Dubrovich, V. K. 1994, *Astron. & Astrophys. Trans.*, 5, 57

Dubrovich, V. K., Lipovka, A. A. 1995, *A&A*, 296, 301

Galli, D. 1990, *Tesi di Dottorato*, Università di Firenze

Galli, D., Palla, F., Ferrini, F., Penco, U. 1995, *ApJ*, 433, 536

Gianturco, F. A., Gori Giorgi, P., Berriche, H., Gadea, F. X. 1996, *A&AS*, 117, 377

Gianturco, F. A., Gori Giorgi, P. 1996a, *ApJ*, in press

Gianturco, F. A., Gori Giorgi, P. 1996b, *Phys. Rev. A*, 54, 1

Goldflam, R., Kouri, D. J., Green, S. 1977, *J. Chem. Phys.*, 67, 5661

Gould, R. J. 1978, *ApJ*, 219, 250

Gunn, J. E., Gott III, R. J. 1972, *ApJ*, 176, 1

Haiman, Z., Thoul, A. A., Loeb, A. 1995, *ApJ*, 464, 523

Huber, K. P., Herzberg, G. 1979 *Molecular Spectra and Molecular Structure. IV. Constants of Diatomic Molecules*, Van Nostrand-Reinhold

Jendrek, E. F., Alexander, M. H. 1980, *J. Chem. Phys.*, 62, 6452

Khersonskii, V. K. 1986, *Astrophysics*, 24, 114

Khersonskii, V. K., Lipovka, A. A. 1993, *Bull. Spec. Astrophys. Obs.*, 36, 88

Kimura, M., Dutta, C. M., Shimakura, N. 1994, *ApJ*, 430, 435

Kirby, K., Dalgarno, A. 1978, *ApJ*, 224, 444

Lahav, O. 1986, *MNRAS*, 220, 259

Lepp, S., Shull, J. M. 1984, *ApJ*, 280, 465

Maoli, R. 1994, PhD Thesis, University of Paris

Maoli, R., Melchiorri, F., Tost, D. 1994, *ApJ*, 425, 372

Maoli, R., Ferrucci, V., Melchiorri, F., Signore, M., Tost, D. 1996, *ApJ*, 457, 1

Mather, J. C. et al. 1993, *ApJ*, 420, 439

Mathews, G. J., Meyer, B. S., Alcock, C. R., Fuller, G. M. 1990, *ApJ*, 358, 36

Palla, F. 1988, in *Galactic & Extragalactic Star Formation*, eds. R. E. Pudritz & M. Fich, Kluwer, p.519

Palla, F., Galli, D., Silk, J. 1995, *ApJ*, 451, 44

Peach, G., Sarah, H. E., Seaton, M. J. 1988, *J. Phys. B*, 21, 3669

Peart, B., Hayton, D. A. 1994, *J. Phys. B*, 27, 2551

Peebles, P. J. E. 1971, *Physical Cosmology*, Princeton University Press

Peebles, P. J. E. 1980, *The Large-Scale Structure of the Universe*, Princeton University Press

Peebles, P. J. E. 1993, *Principles of Physical Cosmology*, Princeton University Press

Pinsonneault, M. H., Deliyannis, C. P., Demarque, P. 1992, *ApJS*, 78, 179

Puy, D., Alecian, J., Le Bourlot, J., Léorat, J., Pineau de Forêts, G. 1993, *A&A*, 267, 337

Ramsbottom, C. A., Bell, K. L., Berrington, K. A. 1994, *J. Phys. B*, 27, 2905

Shu, F. H. 1991 *The Physics of Astrophysics. I. Radiation*, University Science Books

Signore, M., Vedrenne, G., de Bernardis, P., Dubrovich, V., Encrenaz, P., Maoli, R., Masi, S., Mastrantonio, G., Melchiorri, B., Melchiorri, F., Tanzilli, P. E. 1994, *ApJS*, 92, 535

Silver, D. M. 1980, *J. Chem. Phys.*, 72, 6445

Smith, M. S., Kawano, L. H., Malaney, R. A. 1993, *ApJS*, 85, 219

Spite, M., Spite, F. 1982, *Nat.*, 297, 483

Spitzer, L. 1978, *Physical Processes in the Interstellar Medium*, Wiley

Stancil, P. C., Lepp, S., Dalgarno, A. 1996, *ApJ*, 548, 401 (SLD)

Stancil, P. C., Zygelman, B. 1996, *ApJ*, in press

Steigman, G. 1996, *ApJ*, 457, 737

Sunyaev, R. A., Zel'dovich, Ya. B. 1972, *Comments Astrophys. Space Phys.*, 4, 173

Sunyaev, R. A., Zel'dovich, Ya. B. 1980, *MNRAS*, 190, 413

Varshalovich, D. A., Khersonskii, Y. 1977, *Astrophys. Lett.*, 18, 167

van den Bergh, S. 1989, *A&AR*, 1, 111

Verner, D. A., Ferland, G. J. 1996, *ApJS*, 103, 467

Zeldovich, Ya. B. 1978, *SvA Lett.*, 4, 88

Zemke, W. T., Stwalley, W. C. 1980, *J. Chem. Phys.* 73, 5584

APPENDIX A: RADIATIVE TRANSFER IN THE EXPANDING UNIVERSE

The equation of radiative transfer in the expanding Universe can be written as (e.g. Peebles 1971)

$$\frac{1}{c} \frac{dJ_\nu}{dz} = \frac{\kappa_\nu J_\nu - j_\nu}{H_0(1+z)^2\sqrt{1+\Omega_0z}} + \frac{3J_\nu}{c(1+z)}, \quad (A1)$$

where

$$\kappa_\nu = \frac{c^2}{8\pi\nu^2} n_l A_{ul} \frac{g_u}{g_l} \left(1 - \frac{g_l n_u}{g_u n_l}\right) \phi(\nu - \nu_{ul}), \quad (A2)$$

$$j_\nu = \frac{h\nu}{4\pi} n_u A_{ul} \phi(\nu - \nu_{ul}). \quad (A3)$$

Here $\phi(\nu - \nu_{ul})$ is the normalized line-shape function for a transition of frequency ν_{ul} .

In terms of the function $\mathcal{J}_\nu = J_\nu(1+z)^{-3}$, eq. (A1) takes the form

$$\frac{H_0(1+z)^2\sqrt{1+\Omega_0z}}{c\kappa_\nu} \frac{d\mathcal{J}_\nu}{dz} = \mathcal{J}_\nu - \frac{S_\nu}{(1+z)^3}, \quad (A4)$$

where S_ν is the source function defined as

$$S_\nu = \frac{j_\nu}{\kappa_\nu} = \frac{2h\nu^3}{c^2} \left(\frac{g_u n_l}{g_l n_u} - 1 \right)^{-1}. \quad (A5)$$

Eq. (A4) can be formally solved in the usual way multiplying each term for the integrating factor e^τ where

$$\tau_\nu = - \int \frac{c\kappa_\nu}{H_0(1+z)^2\sqrt{1+\Omega_0z}} dz, \quad (A6)$$

obtaining

$$\mathcal{J}_\nu(\tau_\nu) = \mathcal{J}_\nu(0) e^{-\tau_\nu} + e^{-\tau_\nu} \int_0^{\tau_\nu} \frac{S_\nu}{(1+z)^3} e^{\tau'} d\tau'. \quad (A7)$$

Consider now a single transition of frequency ν_{ul} . Absorption of radiation observed today at frequency ν occurs in an interval of the order of the thermal width $\Delta\nu_{th}$ around the line frequency ν_{ul} , or, equivalently, in a range of redshift $\Delta z_i = (1+z_i)\Delta\nu_{th}/\nu_{ul}$ around the “interaction” redshift z_i defined by the condition

$$\nu(1+z_i) = \nu_{ul}. \quad (A8)$$

If the Doppler width of the line is small, as it is the case in the present context, then the size (in redshift) of the interaction region around z_i is also small, and the integral in eq. (A6) can be simplified as

$$\tau(z_i) = \frac{c^3}{8\pi\nu_{ul}^3} A_{ul} \frac{g_u}{g_l} \left[1 - \frac{g_l n_u(z_i)}{g_u n_l(z_i)} \right] n_l(z_i) \left| \frac{dv}{dr} \right|_{z_i}^{-1}, \quad (A9)$$

where

$$\left| \frac{dv}{dr} \right|_{z_i} = H_0(1+z_i)\sqrt{1+\Omega_0 z_i} \quad (\text{A10})$$

is the “cosmological” velocity gradient, due to the expansion of the Universe. The region contributing to the optical depth has a size

$$\Delta\ell = c \frac{dt}{dz} \Delta z_i = \frac{\Delta\nu_{\text{th}}}{\nu_{ul}} \frac{c}{|dv/dr|_{z_i}}. \quad (\text{A11})$$

In the same way, since

$$\int_0^\tau \frac{S_\nu}{(1+z)^3} e^{\tau'} d\tau' = \frac{S_\nu(z_i)}{(1+z_i)^3} [1 - e^{-\tau(z_i)}], \quad (\text{A12})$$

eq. (A7) gives

$$J_\nu[\tau(z_i)] = J_\nu(0)e^{-\tau(z_i)} + e^{-\tau(z_i)} [1 - e^{-\tau(z_i)}] S_\nu(z_i), \quad (\text{A13})$$

and the relative perturbation in the CBR intensity at the present epoch is

$$\frac{\Delta J_\nu}{J_\nu} \Big|_{z=0} = [R(z_i) - 1][1 - e^{-\tau(z_i)}], \quad (\text{A14})$$

where

$$R(z_i) = \left[\frac{g_u n_l(z_i)}{g_l n_u(z_i)} - 1 \right]^{-1} \left\{ \exp \left[\frac{h\nu_{ul}}{kT_r(z_i)} \right] - 1 \right\}. \quad (\text{A15})$$

For a series of transitions of different frequencies $\nu^{(k)}$, the total optical depth at any observed frequency ν is given by the sum $\tau = \sum_k \tau^{(k)}$ of all the single-line contributions $\tau^{(k)}$ evaluated at the redshift of interaction $z_i^{(k)} = \nu^{(k)}/\nu$.

Remember that for black-body radiation the relative distortion in the radiation intensity J_ν , and in the brightness temperature T are related by

$$\frac{\Delta J_\nu}{J_\nu} = \frac{xe^x}{e^x - 1} \frac{\Delta T}{T}, \quad (\text{A16})$$

where $x = h\nu/kT$.

APPENDIX B: RADIATIVE AND COLLISIONAL PROCESSES

The calculation of the level populations of LiH requires the knowledge of radiative and collisional rate coefficients (R_{ij} and C_{ij}) from each state i to any other state j . We have included in our computations only rotovibrational transitions satisfying the selection rules $\Delta v = 0, \pm 1$ for $v = 0\text{--}10$ and $\Delta J = 0, \pm 1$ for $J = 0\text{--}25$.

B1 Radiative processes

Complete tabulations of the Einstein coefficients for vibro-rotational transitions of LiH are not available in the literature. For the sake of completeness and homogeneity, we have computed all the radiative transition probabilities by using the appropriate formulae valid for diatomic molecules in the electric dipole approximation. The rate of spontaneous emission for pure rotational transitions is given by (e.g. Shu 1991)

$$A_{J \rightarrow J-1} = \frac{64\pi^4 \nu_{ul}^3}{3hc^3} D_0^2 \frac{J}{2J+1}, \quad (\text{B1})$$

where $D_0 = 5.888$ debyes (Zemke & Stwalley 1980) is the value of the dipole moment evaluated at the equilibrium separation for the two nuclei. For roto-vibrational transitions,

$$A_{(v, J) \rightarrow (v-1, J \pm 1)} = \frac{8\pi^2 \nu_{ul}^3}{3hc^3 \mu \nu_0} \left(\frac{dD}{dr} \right)_0^2 v f_J, \quad (\text{B2})$$

where

$$f_J = \begin{cases} J/(2J+1) & \text{if } J \rightarrow J-1, \\ (J+1)/(2J+1) & \text{if } J \rightarrow J+1, \end{cases} \quad (\text{B3})$$

$\nu_0 = 1405.65 \text{ cm}^{-1}$ (Huber & Herzberg 1979) is the fundamental frequency of oscillation of LiH, and $(dD/dr)_0 = 0.4132e$ (Zemke & Stwalley 1980) is the derivative of the dipole moment evaluated at the equilibrium position. When a comparison is possible, the Einstein coefficients computed as indicated above agree with the accurate but sparse values tabulated by Zemke & Stwalley (1980) to better than 10%.

The radiative transitions rates R_{ij} can be expressed as function of the corresponding Einstein coefficients A_{ij}

$$R_{ij} = \begin{cases} A_{ij}[1 + \beta_{ij}(T_r)] & \text{if } i > j \\ (g_j/g_i) A_{ji} \beta_{ji}(T_r) & \text{if } i < j \end{cases} \quad (\text{B4})$$

where

$$\beta_{ij} = \left[\exp \left(\frac{E_i - E_j}{kT_r} \right) - 1 \right]^{-1}. \quad (\text{B5})$$

B2 Collisional processes

We consider only excitation and de-excitation of LiH by collision with H atoms, and we factorize $C_{ij} = n(\text{H})\gamma_{ij}$. The cross sections $\sigma_{0,J}$ for the excitation of rotational levels of LiH by collision with He atoms have been calculated by Jendrek & Alexander (1980) on the basis of the potential surface for the (LiH, He) system determined by Silver (1980). These theoretical cross sections are in good agreement with experimental values (Davies 1986). The collisional excitation rates $\gamma_{0,J}(T_g)$ can be obtained from the known cross sections by integrating over a Maxwellian distribution of particle velocities. From the cross sections given by Jendrek & Alexander (1980) we have obtained accurate values of $\gamma_{0,J}$ at $T_g = 3000 \text{ K}$. In order to compute upward rates for generic J and J' we have made use of the infinite order sudden factorisation formula (Goldflam et al. 1977) in the form given by Varshalovich & Khersonskii (1977):

$$\gamma_{JJ'}(T_g) = (2J+1) \sum_{\ell=\ell_1}^{\ell_2} \left(\begin{array}{ccc} J' & \ell & J \\ 0 & 0 & 0 \end{array} \right)^2 \gamma_{0J}(T_g), \quad (\text{B6})$$

where the summation index ℓ assumes integer values between $\ell_1 = |J' - J|$ and $\ell_2 = J' + J$, and the term in parenthesis is a Wigner 3-J symbol. This expression is valid for collision energies much larger than rotational energy spacings.

The corresponding de-excitation rates are then computed by using the principle of detailed balance. The resulting collisional rate coefficients are of the order of $1\text{--}2 \times 10^{-10} \text{ cm}^3 \text{ s}^{-1}$ at $T_g = 3000 \text{ K}$. Since deexcitation cross sections tend to be nearly constant at low energies for collisions between neutral particles (Spitzer 1978), approximate values of $\gamma_{0,J}(T_g)$ at lower temperatures can be obtained by multiplying the de-excitation coefficients at $T_g = 3000 \text{ K}$ by the factor $(T_g/3000 \text{ K})^{1/2}$. An additional factor $\sqrt{3}$ must be adopted to account for the difference in the reduced masses of the (Li,H) and (Li,He) systems.